frontiers in Earth Science

ORIGINAL RESEARCH
published: 13 September 2019
doi: 10.3389/feart.2019.00240

The Response of Magnesium, Silicon, and Calcium Isotopes to Rapidly Uplifting and Weathering Terrains: South Island, New Zealand

Philip A. E. Pogge von Strandmann[1], Katherine R. Hendry[2], Jade E. Hatton[2] and Laura F. Robinson[2]*

[1] London Geochemistry and Isotope Centre, Institute of Earth and Planetary Sciences, University College London and Birkbeck, University of London, London, United Kingdom, [2] School of Earth Sciences, University of Bristol, Bristol, United Kingdom

Silicate weathering is a dominant control on the natural carbon cycle. The supply of rock (e.g., via mountain uplift) has been proposed as a key weathering control, and suggested as the primary cause of Cenozoic cooling. However, this is ambiguous because of a lack of definitive weathering tracers. We use the isotopes of the major cations directly involved in the silicate weathering cycle: magnesium, silicon and calcium. Here we examine these isotope systems in rivers draining catchments with variable uplift rates (used as a proxy for exposure rates) from South Island, New Zealand. Overall, there is no trend between these isotope systems and uplift rates, which is in contrast to those of trace elements like lithium or uranium. Li and Si isotopes co-vary, but only in rapidly uplifting mountainous terrains with little vegetation. In floodplains, in contrast, vegetation further fractionates Si isotopes, decoupling the two tracers. In contrast, Mg and Ca isotopes (which are significantly affected by the weathering of both carbonates and silicates) exhibit no co-variation with each other, or any other weathering proxy. This suggests that lithology, secondary mineral formation and vegetation growth are causing variable fractionation, and decoupling the tracers from each other. Hence, in this context, the isotope ratios of the major cations are significantly less useful as weathering tracers than those of trace elements, which tend to have fewer fractionating processes.

Keywords: weathering (IGC: D3/D5/D6), climate, uplift (IGC: e3/h3), isotope, mountains

OPEN ACCESS

Edited by:
Xiao-Ming Liu, University of North Carolina at Chapel Hill, United States

Reviewed by:
Christopher Robert Pearce, University of Southampton, United Kingdom
Shui Jiong Wang, China University of Geosciences, China

****Correspondence:***
Philip A. E. Pogge von Strandmann
p.strandmann@ucl.ac.uk

Specialty section:
This article was submitted to Geochemistry, a section of the journal Frontiers in Earth Science

Received: *14 June 2019*
Accepted: *30 August 2019*
Published: *13 September 2019*

Citation:
Pogge von Strandmann PAE, Hendry KR, Hatton JE and Robinson LF (2019) The Response of Magnesium, Silicon, and Calcium Isotopes to Rapidly Uplifting and Weathering Terrains: South Island, New Zealand. Front. Earth Sci. 7:240. doi: 10.3389/feart.2019.00240

INTRODUCTION

Chemical weathering of silicate rocks is a dominant controlling process on atmospheric CO_2 concentrations, on timescales ranging from the seasonal to the multi-millennial. On short timescales, weathering provides nutrients (such as P, Fe, K, etc.) for the growth of organic carbon in coastal waters, and, critically, also the clay particles and highly reactive iron that assists in organic carbon burial (Lalonde et al., 2012; Schrumpf et al., 2013; Barber et al., 2014; Hawley et al., 2017). On longer timescales, the more "traditional" aspect of silicate weathering comes into play, which is the transport of bicarbonate and carbonate-forming cations (e.g., Ca and Mg) from the continents to the oceans, where they sequester carbon by precipitating marine carbonates (Walker et al., 1981; Berner et al., 1983; Berner, 2003). Because of this, there is significant interest in determining

and quantifying the processes that control silicate weathering. These broadly divide into two endmembers, which consist of a climate-based control (via temperature and the hydrological cycle) on weathering rates (Berner et al., 1983; Gíslason et al., 2006; Gislason et al., 2009), and (instead of temperature) a rock supply-driven control on weathering rates (Raymo et al., 1988; Raymo and Ruddiman, 1992; Hilley et al., 2010). The former would provide a feedback mechanism that would act to stabilize the climate, while the latter provides a method to change the equilibrium climate state. It generally appears that different weathering regimes exist in different terrains and climates (West et al., 2005), making it difficult to determine the overarching controls.

One of the key time periods for which these controls are debated is the Cenozoic, where it has been proposed that cooling was caused by enhanced weathering rates due to Himalayan uplift (Raymo and Ruddiman, 1992; Misra and Froelich, 2012), although this hypothesis remains controversial. It is certainly difficult to reconcile Cenozoic marine carbonate isotope records (e.g., Sr, Os, and Li; Ravizza, 1993; McArthur et al., 2001; Hathorne and James, 2006) with the uplift of a single mountain belt from the mass balance perspective (Li and West, 2014; Wanner et al., 2014). One method for testing the impact of rapidly uplifting mountain belts on weathering in the past is to examine modern analogs. South Island, New Zealand provides such a rapidly uplifting terrain. Usefully, the different sides of the island have very different uplift rates, with the west coast representing mountainous terrains, while the east coast represents a much flatter floodplain (Robinson et al., 2004). In particular, uplift rates were determined for individual sample areas by Robinson et al. (2004), and used as a proxy for the exposure rate of fresh rock. This study takes a multi-tracer approach to examining the weathering processes in this natural laboratory. We use the isotopes of elements directly involved in the silicate weathering and carbon cycle, namely magnesium, silicon and calcium. We combine these with previously measured trace element isotope ratios which have been shown to reflect different aspects of weathering processes: uranium isotopes (Robinson et al., 2004) and lithium isotopes (Pogge von Strandmann and Henderson, 2015). In both cases, Li and U isotopes formed correlations with the uplift (or exposure) rate, demonstrating that these trace elemental proxies can provide useful information on weathering and the carbon cycle.

Magnesium is an element directly involved in the carbon cycle, via weathering of Mg-silicates, precipitation of Mg-rich carbonates (both dolomites and high-Mg calcites) and the exchange of Ca for Mg at mid-ocean ridges (Holland, 2005). Therefore Mg isotopes have the potential to provide information on weathering (Tipper et al., 2006b, 2012a; Pogge von Strandmann et al., 2008, 2014a, 2019b; Foster et al., 2010; Higgins and Schrag, 2010; Teng et al., 2010; Opfergelt et al., 2014; Chapela Lara et al., 2017). However, the study of global rivers has revealed a large range in dissolved Mg isotope ratios (Tipper et al., 2006a, 2008, 2010, 2012a,b; Brenot et al., 2008; Pogge von Strandmann et al., 2008, 2012; Wimpenny et al., 2011; Huang et al., 2012; Liu et al., 2014; Teng, 2017; Oelkers et al., 2019a), and it has become clear that, like all major elements, Mg and its isotopes are affected by a wide range of processes. The balance of carbonate to silicate in a catchment plays a significant role, with carbonates being isotopically lighter and more isotopically variable than silicates (Tipper et al., 2006a,b, 2008, 2012a; Hippler et al., 2009; Wombacher et al., 2011; Pogge von Strandmann et al., 2014a, 2019b). In addition, Mg isotopic fractionation occurs due to the silicate weathering process itself, owing to both preferential incorporation and adsorption of Mg isotopes by secondary minerals (Pogge von Strandmann et al., 2008, 2012; Huang et al., 2012; Opfergelt et al., 2012a, 2014; Tipper et al., 2012a; Liu et al., 2014; Oelkers et al., 2019a). Finally, the uptake of Mg by plants causes variable isotope fractionation (Black et al., 2006; Bolou-Bi et al., 2010, 2012).

Silicon is another element directly involved in silicate weathering and the carbon cycle. In principle, silicon isotope behavior during weathering is simpler than that of Mg isotopes, given that Si is dominated by silicate weathering. The formation of secondary silicate and adsorption of dissolved Si onto iron oxy-hydroxides (Delstanche et al., 2009) are both associated with the preferential uptake of light isotopes, driving river waters and seawater to isotopically heavier values that the initial primary silicate rock (De la Rocha et al., 2000; Ziegler et al., 2005; Georg et al., 2006a, 2007; Opfergelt et al., 2009, 2013; Pogge von Strandmann et al., 2012, 2014b; Frings et al., 2015, 2016; Hatton et al., 2019). Dissolution of secondary weathering products will, in turn, release the lighter isotopes back into solution (Fontorbe et al., 2013). In addition, primary productivity (e.g., diatoms) and plant growth exert an influence, and preferentially take up light isotopes (Opfergelt et al., 2006).

The final major cation directly involved in the carbon cycle is calcium. There are similarities between Ca isotopes and Mg isotopes, in that both are controlled by the dissolution of isotopically light carbonates and isotopically heavy silicates, as well as the precipitation of silicate secondary minerals and plant growth (Tipper et al., 2006a, 2008; Farkaš et al., 2007; Hindshaw et al., 2013; Moore et al., 2013; Fantle and Tipper, 2014; Kasemann et al., 2014; Jacobson et al., 2015; Perez-Fernandez et al., 2017). However, Ca isotopes tend to be harder to unambiguously interpret, because the isotopic range in carbonates and silicates are relatively wider than for Mg isotopes, and far closer (and overlapping) in isotopic space (Fantle and Tipper, 2014). Nevertheless, Ca isotopes have been used to examine weathering processes in the geological record (Kasemann et al., 2005, 2008, 2014; Farkaš et al., 2007; Blättler et al., 2011; Holmden et al., 2012; Fantle and Tipper, 2014), as well as quantification of carbonate precipitation rates (Pogge von Strandmann et al., 2019a).

Here we examine the Mg, Si and Ca isotope ratios from rivers from South Island, New Zealand, to test whether the isotopes of the major elements can provide useful information on weathering regimes, especially when comparing to trace element isotope ratios.

FIELD AREA

Rivers were sampled from multiple catchments around South Island, New Zealand, divided between the East and West of the island (**Figure 1**; Robinson et al., 2004). In general, the individual catchment areas are small, so rivers flow through

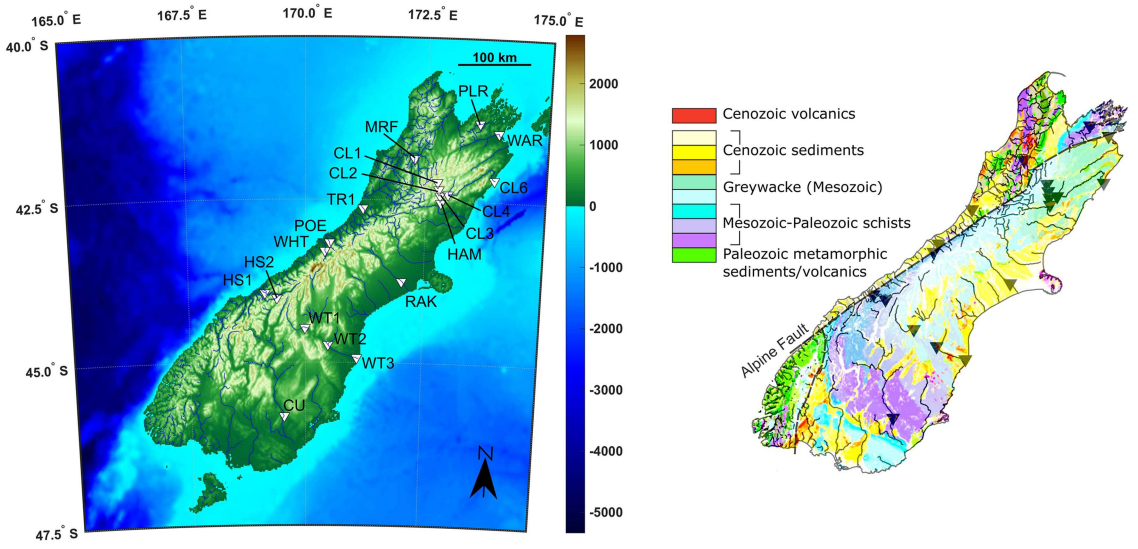

FIGURE 1 | Sample location topographical map and geological map (Geological Map of New Zealand, 2012). The Cenozoic sediments are a mixture of volcanoclastics, conglomerates, sandstones, and siltstones. Both datasets are licensed under a Creative Commons Attribution 4.0 International Public License.

a relatively narrow range of rainfall and uplift environments. Robinson et al. (2004) developed a hydrologically accurate digital elevation model, which allows estimates of the average rainfall and uplift rate for each catchment, by using digitized rainfall and uplift maps (**Table 1**). The western coast has significantly more rainfall than the east (an average of 8,000 compared to 1,600 mm/year), and a higher uplift rate (5.8 ± 1.5 compared to 1.9 ± 0.8 mm/year). Overall there is a positive correlation ($r^2 = 0.61$) between uplift and rainfall, and uplift/rainfall ratios are higher in the East. Hydrothermal springs were sampled at Hanmer Springs, to assess the effects of hydrothermal processes, although these springs do not drain into any of the studied rivers. The weathering lithologies are relatively complex, but are dominantly comprised of Mesozoic graywackes and schists (Jacobson and Blum, 2003; Jacobson et al., 2003). Most rivers drain these lithologies (**Figure 1**), with some, largely at the coast, also having some input from Cenozoic sediments, which mainly consist of siliciclastics of various grain sizes (Geological Map of New Zealand, 2012). The primary lithology of each sample is given in **Table 1**.

As well as splitting samples into being from the East and West coasts, we also examine areas by vegetation type. Very broadly, and detailed in **Table 1**, we can divide into three main vegetation types: (1) glacial, permanent snow or rock with native forests, which largely coincides with the samples from the west coast; (2) shrubs or bare ground, which coincides with east coast samples from the Clarence River, and (3) dry open grassland.

METHODS

All data are reported in **Table 1**. Elemental concentrations were measured by quadrupole ICP-MS, as described in Pogge von Strandmann and Henderson (2015). We have since reassessed the Si concentrations (which tend to have relatively poor accuracy and precision using ICP-MS). Dissolved Si (DSi) concentrations were determined spectrophotometrically using a Hach Lange DR3900 (Ultra Low Range Method 8186). Accuracy and precision (±1 and ±3%, respectively) were assessed using repeat measurements of a standard solution and duplicate sample measurements. The DSi concentrations reported in **Table 1** are therefore the updated concentrations.

In addition, three new samples were analyzed for elemental concentrations and Si isotopes. These samples were collected during the sampling campaign of Robinson et al. (2004), but were not analyzed for U isotopes or uplift patterns in that study. For these samples, elemental concentrations were determined by analytical triplicate measurements by ICP-OES at the University of Bristol, calibrated against certified multi-element standard solutions, with precision of <0.2, <0.02, <0.07 ppm for Ca, K, Mg, and Na, respectively (1sd).

Mg Isotopes

Mg isotope were purified by passing samples through a two-column procedure using AG50W X-12 cation exchange resin, using 2 M HNO_3 as an eluent. Splits were collected either side of the main collection bracket and independently checked for Mg concentrations. These splits contained <0.01% of the sample's Mg, showing that >99.9% of Mg was collected. Samples were analyzed at the Bristol Isotope Group, using a Thermo Neptune MC-ICP-MS, following the procedures outlined elsewhere (Pogge von Strandmann et al., 2011b, 2012, 2019b). The accuracy and precision of this method can be demonstrated by a number of inter-laboratory comparison studies on different standard types, as well as standard compilations (Foster et al., 2010; Teng et al., 2015; Shalev et al., 2018). Seawater measured alongside the analyses made during this study give $\delta^{26}Mg = -0.83 \pm 0.05$ (2sd,

TABLE 1 | Elemental concentrations (from Pogge von Strandmann and Henderson, 2015) and isotope ratios for the New Zealand rivers.

	River	Latitude	Longitude	Uplift rate (mm/year)	Rainfall (mm/year)	Vegetation	Primary lithology	Li (nmol/l)	Na (μmol/l)	Mg (μmol/l)	Al (μmol/l)	Si (μmol/l)	K (μmol/l)	Ca (μmol/l)	δ^7Li	δ^{26}Mg	2se	δ^{44}Ca	2se	δ^{30}Si	(^{234}U/^{238}U)
EAST																					
CL1	Clarence	S 42° 12′ 53.6	E 172° 44′ 28.5	2.3	1,280	Shrubs, tussock, bare ground	Greywacke	167	31.4	1.76	13.2	74.1	3.19	148	22.0	−0.74	0.03	0.90	0.08	0.89	2.577
CL2	Clarence	S 42° 19′ 32.7	E 172° 46′ 14.4	2.1	1,194		Greywacke	85.5	20.2	7.28	11.9	104	4.45	243	28.3	−0.66	0.04			1.25	2.774
CL3	Clarence	S 42° 25′ 24.5	E 172° 47′ 44.6	2.1	1,136		Greywacke	35.3	19.0	5.71	4.10	117	4.22	208	34.7	−0.67	0.04	0.93	0.09	0.79	2.548
CL4	Clarence	S 42° 24′ 00.1	E 172° 57′ 36.7	2.2	1,114		Greywacke	44.6	23.9	12.7	13.6	125	7.96	404	26.2	−0.68	0.04			0.96	2.519
CL6	Clarence mouth	S 42° 09′ 51.3	E 173° 54′ 42.7	3.7	938	Dry open grassland or grass/shrub mosaic	Greywacke	290	35.3	12.2	4.09	140	7.55	212	22.6	−0.72	0.04	0.58	0.06	1.07	2.861
WT2	Waitaki	S 44° 43′ 55.5	E 170° 28′ 42.0	1.5	2,378		Greywacke	66.9	11.2	3.21	1.37	78.9	2.23	150	24.9	−0.53	0.04	0.54	0.07	1.29	1.316
WT3	Waitaki	S 44° 55′ 38.5	E 171° 06′ 04.4	1.2	2,014		Cenozoic sediments	83.6	11.6	4.16	3.50	65.3	3.06	196	25.9	−0.70	0.03			0.96	1.297
WT1	Waitaki	S 44° 28′ 19.4	E 169° 59′ 15.5	0.6	1,317		Greywacke	50.2	26.7	10.2	7.91	122	10.0	285	30.7	−0.75	0.04	0.97	0.01	0.78	1.500
RAK	Rakaia	S 43° 45′ 09.2	E 172° 01′ 49.8	2.1	3,320		Cenozoic sediments	115	14.9	10.8	11.4	94.0	3.70	351	27.2	−0.65	0.03			1.00	1.411
WAR	Wairau	S 41° 26′ 39.3	E 173° 58′ 02.3	1.8	1,129		Cenozoic sediments	225	23.8	9.17	3.9	147	2.95	206	22.3	−0.65	0.02			1.12	1.946
CU	Clutha	S 45° 49′ 34.4	E 169° 31′ 52.3	1.1	1,556		Schist	59.7				61.4			26.3	−0.44	0.02	0.70	0.06	1.37	1.081
	rpt																			1.34	
WA1	Waiau						Cenozoic sediments					125								1.26	
WEST																					
TR1	Taramakau	S 42° 37′ 58.1	E 171° 11′ 59.7	5.2	5,283		Cenozoic sediments	136	47.7	15.6	15.5	103	20.1	412	24.5	−0.62	0.02	0.86	0.08	0.94	1.092
POE	Poerua	S 43° 09′ 39.6	E 170° 30′ 17.2	7.4	6,300	Glacier/permanent snow, rock	Cenozoic sediments	386	10.6	5.66	4.91	96.5	9.54	206	13.2	−0.85	0.03	1.06	0.07	0.61	1.232
HS2	Haast	S 44° 00′ 56.8	E 169° 23′ 01.7	4.3	8,924		Schist	44.6	15.5	6.07	4.03	46.3	5.63	210	23.6	−0.61	0.05	0.82	0.07	0.83	1.171
	rpt																			0.66	
HS1	Haast	S 43° 56′ 11.5	E 169° 07′ 43.7	4.8	10,063		Schist	124	28.1	8.93	4.01	59.0	13.3	216	18.7	−0.51	0.01	0.77	0.08	0.76	1.185
WHT	Whataroa	S 43° 17′ 20.5	E 170° 24′ 13.5	7.4	9,277		Schist	539	33.7	4.00	19.6	114	6.64	153	7.6	−0.52	0.04	1.40	0.03	0.09	1.158
	rpt																	1.34	0.07		
MRF	Maruia falls						Schist					139								0.98	
PLR	Pelorus river						Schist					214								1.23	
	Hanmer springs	S 42° 32′	E 172° 49′					121000							5.8	−2.18	0.03			−1.31	1.416
	rpt																			−1.33	

Lithium and uranium isotope ratios are from Pogge von Strandmann and Henderson (2015) and Robinson et al. (2004). External (long-term) analytical uncertainty is ±0.5‰ on δ^7Li, ±0.07‰ on δ^{26}Mg, ±0.15‰ on δ^{30}Si and ±0.14‰ on δ^{44}Ca.

$n = 3$), in keeping with the long-term values and precision. The long-term external analytical uncertainty using this method is ±0.07‰ (2sd) on δ^{26}Mg.

Si Isotopes

Sample solutions were filtered (0.2 micron Pall Acrodisc) and then purified by passing through pre-conditioned AG50W X-12 cation exchange resin, and eluting with 18 MΩ.cm Milli-Q water to produce a final solution of 2 ppm Si (Georg et al., 2006b). The samples were spiked with an intensity-matched Mg solution to correct for internal mass bias and 100 µl of 0.1 M H_2SO_4 (Romil UpA) to account for potential anionic matrix mass bias (Cardinal et al., 2003; Hughes et al., 2011). The samples were then analyzed for all stable Mg and Si isotopes at the Bristol Isotope Group, using a Thermo Neptune MC-ICP-MS, following the procedures outlined elsewhere (Hatton et al., 2019). Machine blank, Mg mass bias and standard-sample bracketing (relative to NBS28/RM8546) corrections were all carried out offline. Replicate measurements of reference standard Diatomite and sponge specimen LMG08 yielded values of $\delta^{29}Si = +0.64 \pm 0.11$‰; $\delta^{30}Si = +1.25 \pm 0.15$‰ (2sd; $n = 35$) and $\delta^{29}Si = -1.76 \pm 0.11$‰; $\delta^{30}Si = -3.41 \pm 0.15$ ‰ (2sd, $n = 59$), respectively, in good agreement published interlaboratory comparisons (Reynolds et al., 2007; Hendry et al., 2011). Replicate measurements of a freshwater standard from the Natural Environment Research Council (NERC) Isotope Geosciences Laboratory gave an average value of $\delta^{29}Si = +0.46 \pm 0.06$‰ and $\delta^{30}Si = 0.91 \pm 0.08$‰ (2sd; $n = 3$) in good agreement with previous literature values (Panizzo et al., 2016). Full duplicate sample δ^{30}Si measurements all agreed within ± 0.08‰. The δ^{29}Si and δ^{30}Si values for all standards and samples were linearly related, with a gradient of 0.5126 ± 0.0073 (95% confidence), which lies between kinetic and thermodynamic equilibrium mass-dependent fractionation. The long-term external analytical uncertainty using this method is ±0.15‰ (2sd).

Ca Isotopes

Around 10 µg of calcium was purified through a two-stage column procedure, the first column containing AG50 X12 resin, which removes most matrix elements, and the second containing Sr-spec resin, which removes any Sr. Splits collected before and after the Ca elution peak contained <0.5% of the Ca, indicating column yields of >99.5%. Analyses were performed on a Nu Instruments MC-ICP-MS at Oxford, relative to the standard SRM-915a. Sr isobaric interference was monitored at mass 43.5, and used to correct the ^{42}Ca, ^{43}Ca, and ^{44}Ca intensities. This column and mass spectrometric methodology has been detailed in a series of studies (Halicz et al., 1999; Reynard et al., 2010; Blättler et al., 2011; Perez-Fernandez et al., 2017; Pogge von Strandmann et al., 2019a). Seawater measured by this method yields $\delta^{44/40}$Ca values of 1.92 ± 0.14‰ (2sd, $n = 16$), in keeping with other studies (Hippler et al., 2003; Hindshaw et al., 2013), giving a long-term external analytical uncertainty of ±0.14‰.

RESULTS

All of the river waters plot along a mixing line between Ca/Na and Mg/Na ratios (Pogge von Strandmann and Henderson, 2015), broadly implying mixing between silicate and carbonate endmembers. Previously analyzed rivers from South Island (Jacobson et al., 2003) are reported to be dominated by weathering reactions involving plagioclase and calcite, with kaolinite the dominantly forming clay mineral (together with minor amounts of smectite).

Magnesium concentrations range between ∼2 and 164 µmol/l, spanning both the range shown by global large rivers (Gaillardet et al., 1999), but also the range shown by mountainous rivers from New Zealand itself (Jacobson et al., 2003), as well as the Himalayas (Tipper et al., 2008) or glaciated rivers from Iceland (Pogge von Strandmann et al., 2008). Mg isotope ratios (δ^{26}Mg) range between −0.85 and −0.44‰, somewhat isotopically heavier (and closer to the composition of silicate rocks) than the global riverine mean of −1.09‰ (Tipper et al., 2006b).

Dissolved silicon (DSi) concentrations range between 61 and 214 µmol/l, also on the low side of the global riverine range (Frings et al., 2015, 2016), but similar to those previously measured from New Zealand (Jacobson et al., 2003). The δ^{30}Si values range between 0.09 and 1.39‰, plotting about the riverine mean of 1.25 ± 0.68‰ (Frings et al., 2016).

Calcium concentrations range between 135 and 412 µmol/l, generally at the lower end of the range of global rivers

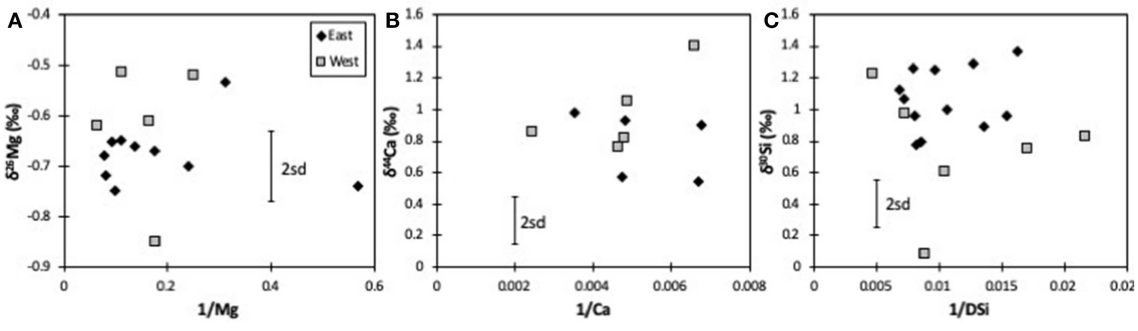

FIGURE 2 | Mixing plots for Mg **(A)**, Ca **(B)**, and Si isotopes **(C)**. Concentrations are in 1/µM. The error bars represent the long-term 2sd external uncertainty.

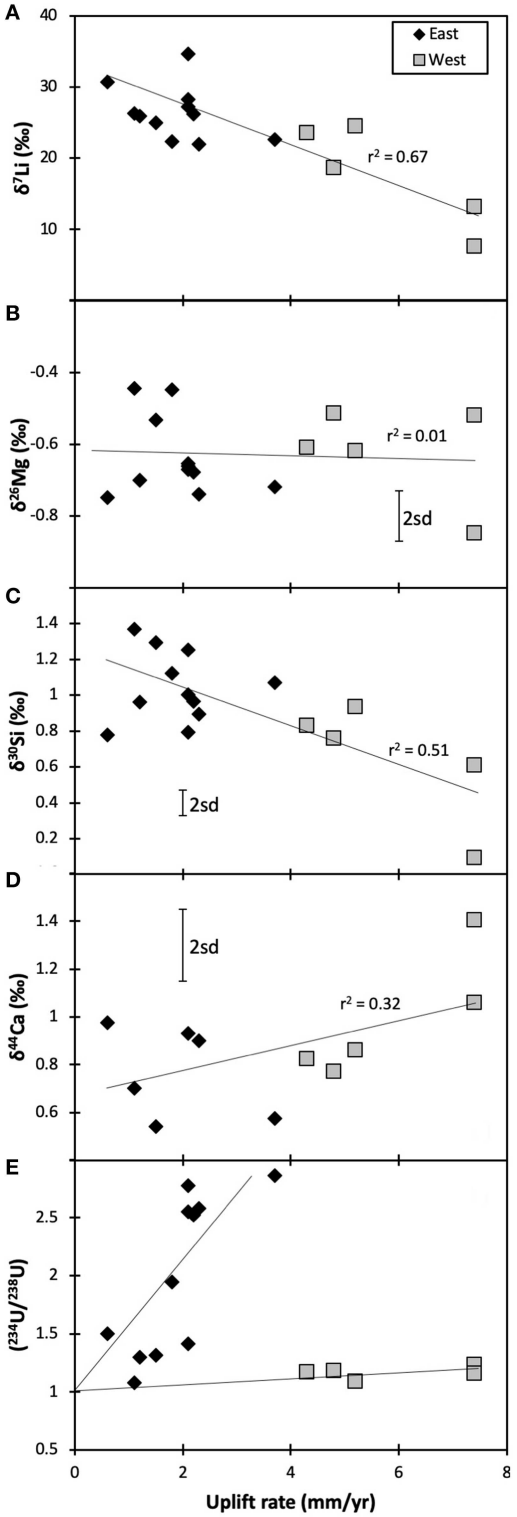

FIGURE 3 | Isotope ratios of Mg **(B)**, Si **(C)**, and Ca **(D)** plotted against uplift rates, which are used as a proxy for fresh rock exposure rates. The trends of Li [**(A)**; Pogge von Strandmann and Henderson, 2015] and U isotopes [**(E)**; Robinson et al., 2004] relative to uplift rates are also shown. Overall, the figure suggests that isotopes of trace elements may provide more weathering information than those of major elements. The error bars represent the long-term 2sd external uncertainty.

(Gaillardet et al., 1999), but similar to previously measured rivers from New Zealand (Jacobson et al., 2003). Riverine $\delta^{44/40}$Ca values range from 0.54 to 1.40‰, also around the global mean riverine value of 0.88‰ (Fantle and Tipper, 2014). Ca isotope ratios from our rivers are similar to the range reported from rivers in the center of South Island of 0.5–1‰ (Moore et al., 2013).

The hydrothermal Hanmer Springs was analyzed for several different isotopic systems to assess the effects of hydrothermal processes, although these springs do not drain into any of the studied rivers. The Mg isotope ratio is highly fractionated (δ^{26}Mg of −2.2‰), in keeping with the analyses of other hot springs (Pogge von Strandmann et al., 2019b). Mg is typically removed from solutions during hydrothermal exchange into secondary minerals (Holland, 2005), causing significant isotope fractionation. Silicon isotopes are also highly fractionated (δ^{30}Si = −1.3‰) from bedrock values [∼-0.29‰ Savage et al., 2010], but in this case to values significantly lighter than the bedrock. Previous δ^{30}Si measurements of hydrothermal fluids, including hot springs, range from ∼-0.5 to 0.5‰ (Ding et al., 1996; Opfergelt et al., 2013; Geilert et al., 2015). The light value measured here suggests that some other process is driving this system toward lighter isotopic compositions, such as the dissolution of secondary minerals or siliceous precipitates (Geilert et al., 2015). In comparison, the δ^{7}Li value is 5.8‰, which is similar to primary silicate rocks (Pogge von Strandmann and Henderson, 2015).

DISCUSSION

Riverine Magnesium

Generally, riverine Mg isotopes tend to represent mixing between the dissolution of isotopically heavy silicates (δ^{26}Mg ∼ −0.2‰) and isotopically light carbonates (δ^{26}Mg = −5 to −0.5‰) (Teng, 2017). Carbonate precipitation can therefore drive waters isotopically heavy (Pogge von Strandmann et al., 2019b). There is also an added fractionation effect by the formation of silicate secondary minerals, which mainly tend to preferentially take up heavy Mg isotopes, driving rivers waters isotopically lighter (Tipper et al., 2006a, 2008, 2012a; Brenot et al., 2008; Pogge von Strandmann et al., 2008, 2012; Huang et al., 2012; Lee et al., 2014; Opfergelt et al., 2014; Chapela Lara et al., 2017). Plants also fractionate Mg isotopes with a variable fractionation direction, although with a general enrichment in heavy isotopes (Black et al., 2006; Bolou-Bi et al., 2010, 2012).

For Mg isotopes, both the mountainous West and the flatter East coasts have a similar isotopic range, and an identical average [δ^{26}Mg = −0.62 ± 0.14 (n = 5) vs. −0.64 ± 0.11‰ (n = 11), respectively]. There is also no obvious difference between rivers with different primary lithologies (δ^{26}Mg = −0.68 ± 0.07‰, n = 7 for greywacke; −0.52 ± 0.07‰, n = 4 for schist; −0.69 ± 0.09‰, n = 5 for Cenozoic sediments; **Table 1**). Equally, Mg isotope ratios show no mixing trend between endmembers (**Figure 2A**), further suggesting no overarching simple control by lithology. During chemical weathering Na is the most mobile major cation, meaning that it has the lowest tendency to be taken up into secondary minerals. Mg/Na ratios should therefore provide information on dissolution of primary minerals vs.

formation and uptake by secondary minerals. However, unlike the isotope ratios of trace elements such as lithium (Pogge von Strandmann et al., 2017; Murphy et al., 2019), we do not observe a simple relationship between δ^{26}Mg and Mg/Na or Ca/Mg for either coast, which is not necessarily to be expected, given the variable isotope ratios of both silicates and carbonates. Similarly, there is no relationship between δ^{26}Mg and the ratio of divalent to monovalent cations, which has also been used as a proxy for silicate weathering (Tranter et al., 2002; Hatton et al., 2019). Given that silicate and carbonate dissolution have been reported to largely control the elemental composition of New Zealand rivers (Jacobson and Blum, 2003; Jacobson et al., 2003), this lack of correlation would imply that Mg isotopes are not only controlled by mixing between silicate and carbonate dissolution, but also by formation of silicate secondary minerals, which preferentially take up heavy Mg isotopes, and by Mg uptake by plants (Tipper et al., 2006a,b, 2008; Bolou-Bi et al., 2010, 2012). In addition, Mg in these rivers is also variably sourced from rainwater, which largely derives from seawater (Jacobson et al., 2003), and hence would have a δ^{26}Mg = −0.82‰ (Foster et al., 2010). There is no trend between δ^{26}Mg and rainfall amount, and indeed the sample with the highest rainfall (HS1 with >10,000 mm/year; Robinson et al., 2004) has a δ^{26}Mg much higher than that of seawater (−0.51‰, compared to −0.82‰, respectively).

Interestingly, despite all these potential variations, the δ^{26}Mg of these rivers has a relatively narrow range of 0.4‰, and the absolute δ^{26}Mg values (−0.45 to −0.85‰) are relatively close to those of silicates (−0.23‰) (Pogge von Strandmann et al., 2011b; Hin et al., 2017; Teng, 2017). Overall, then, Mg is largely sourced from silicate dissolution in these rivers, given that both rainwater contribution and clay formation would drive dissolved

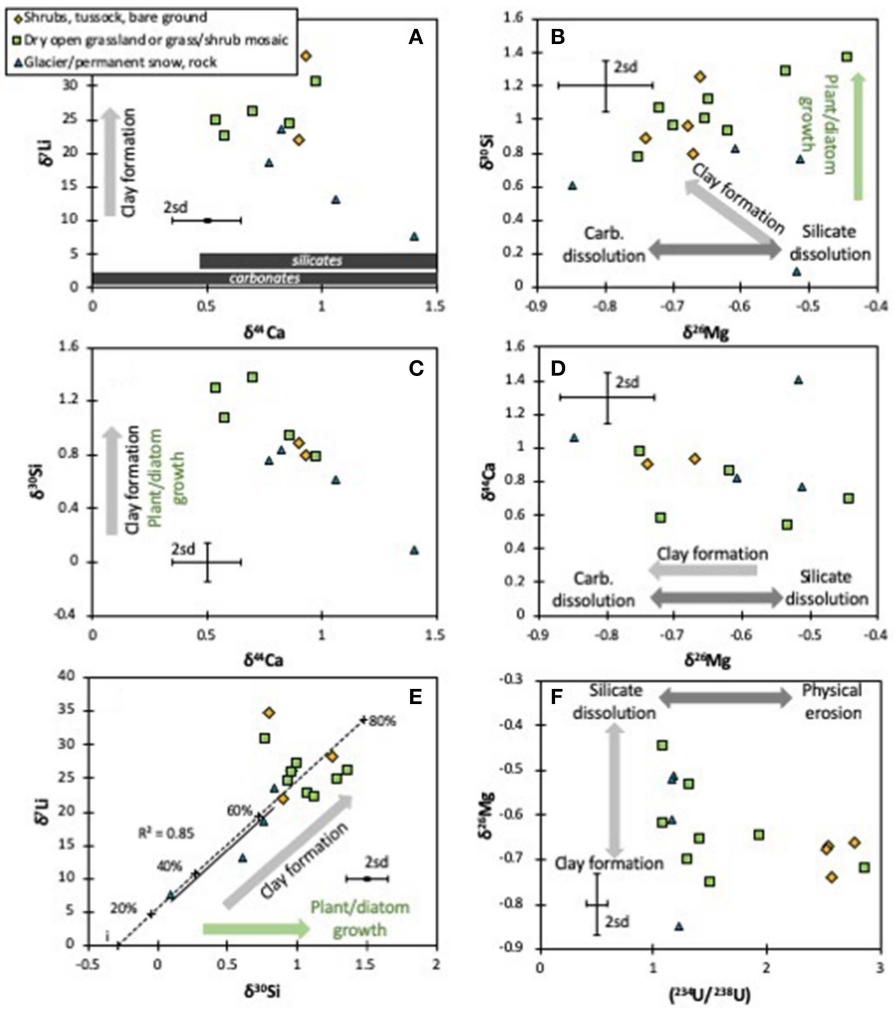

FIGURE 4 | Cross-plots between the isotope systems analyzed in this and other studies for the different vegetation types (Robinson et al., 2004; Pogge von Strandmann and Henderson, 2015): isotopes of Li vs. Ca **(A)**, Si vs. Mg **(B)**, Si vs. Ca **(C)**, Ca vs. Mg **(D)**, Li vs. Si **(E)** and Mg vs. U **(F)**. The arrows represent fractionation directions by different weathering and plant formation processes. For Ca isotopes **(A)**, the range of carbonate and silicate rocks is shown. The error bars represent the long-term 2sd external uncertainty.

δ^{26}Mg to even lower values (i.e., further toward the composition of carbonates).

The fairly constant δ^{26}Mg values in the rivers suggest that the sources of Mg remain relatively unchanged across South Island, and hence there is no relationship between δ^{26}Mg and the uplift rate (used here as a proxy for exposure rate—**Figure 3B**). Hence, unsurprisingly, the simple ratio of silicate rock supply vs. clay formation that control lithium isotopes and result in a negative co-variation of δ^{7}Li and uplift rates (**Figure 3A**) (Pogge von Strandmann and Henderson, 2015), do not control Mg behavior. Equally, there is no co-variation between δ^{26}Mg and tracers of either clay formation (Li and Si isotopes, **Figure 4B**), plant growth (Si and Ca isotopes, **Figure 4D**) or lithology (Ca isotopes). These other isotope systems are discussed below.

There is, however, an interesting relationship between δ^{26}Mg and (^{234}U/^{238}U) (**Figure 4F**). When the U activity ratio is low (close to secular equilibrium) the Mg isotope ratios are highly variable, whereas when (^{234}U/^{238}U) is high (>1.5), δ^{26}Mg values are fairly constant at ∼-0.7‰. There is no apparent influence by vegetation, as both glacial and vegetated terrains cover the entire range of observed δ^{26}Mg. Uranium activity ratios are controlled by the ratio of physical erosion to mineral dissolution (Henderson, 2002; Chabaux et al., 2003; Robinson et al., 2004; Pogge von Strandmann et al., 2006, 2010, 2011a; Andersen et al., 2009; Hindshaw et al., 2018). Relatively high physical erosion rates increase mineral surface area, promoting both recoil of ^{234}U and the leaching of ^{234}U from recoil-damaged lattice sites, and driving riverine (^{234}U/^{238}U) to high values (**Figure 3E**). In contrast, relatively high dissolution rates will drive river water (^{234}U/^{238}U) toward the secular equilibrium value of 1, the value of the bulk silicate rock. In other words, when chemical dissolution is relatively high [(^{234}U/^{238}U) close to secular equilibrium], silicate dissolution drives δ^{26}Mg toward the relatively heavy isotope ratio of silicates. In contrast, when water-rock contact times are long (in the flatter floodplain areas in the east of South Island) there is relatively greater clay formation, which on average impose an isotopic fractionation factor of ∼0.5‰ (Wimpenny et al., 2014), hence driving riverine δ^{26}Mg to values ∼0.5‰ lower than silicate rock. As such, there does appear to be a secondary mineral control on Mg isotopes that is, however, not directly comparable to the secondary minerals that control Li or Si isotopes, given the lack of co-variations. This may be due to the composition of the secondary minerals, in that the primary clay mineral, kaolinite (Jacobson et al., 2003), does not contain Mg as a major constituent, meaning that Mg isotopes may be at least partly controlled by fractionation during adsorption (Pogge von Strandmann et al., 2012).

Riverine Silicon

Riverine Si isotopes are controlled by the ratio of silicate dissolution (causing low isotope ratios) to clay or amorphous silicate precipitation (driving riverine δ^{30}Si high) (De la Rocha et al., 2000; Opfergelt et al., 2012b, 2017; Pogge von Strandmann et al., 2012; Frings et al., 2015; Hatton et al., 2019). In addition, uptake of Si by plants or plankton drives the residual river water Si toward heavy values as a result of preferential uptake of lighter isotopes into biogenic silica (De la Rocha et al., 1997; Opfergelt et al., 2011).

All riverine dissolved Si isotope ratios in the New Zealand rivers are isotopically heavier than the bedrock (Savage et al., 2010). While some subglacial rivers in Greenland have δ^{30}Si values that are lower than the bedrock (and are interpreted as the dissolution of secondary weathering products, a process also observed in groundwaters) (Georg et al., 2009; Pogge von Strandmann et al., 2014b; Hatton et al., 2019), most glacial and non-glacial rivers are, like these New Zealand rivers, isotopically heavier than the bedrock due to clay formation (Georg et al., 2006a, 2007; Cardinal et al., 2010; Opfergelt et al., 2012b, 2013; Pogge von Strandmann et al., 2012; Fontorbe et al., 2013). The flatter east coast shows very little δ^{30}Si variability for a fairly wide range in Si/Na, Si/(Na + K), and DSi concentrations. As such, there is no obvious mixing relationship between clear endmembers (**Figure 2B**).

There is a relatively weak negative relationship between δ^{30}Si and the uplift rate (**Figure 3C**; $r^2 = 0.51$, significant $p < 0.05$, Spearman Rank correlation), which is here used as a proxy for the exposure rate of fresh rock (Robinson et al., 2004; Pogge von Strandmann and Henderson, 2015). The lithium isotope ratio, which also traces silicate weathering, also shows a correlation with uplift rate, although it is much stronger ($r^2 = 0.67$, significant $p < 0.01$; **Figure 3A**) (Pogge von Strandmann and Henderson, 2015). In both cases a higher exposure rate of fresh rock in mountainous areas drives the isotope ratio closer to that of silicate rock. In contrast, the longer fluid-rock contact times that occur in the flatter floodplains promote the formation of clay minerals and CO_2 drawdown (West et al., 2002). The weaker correlation with uplift rates for Si isotopes compared to Li isotopes is likely because of the additional effect of plants and freshwater diatoms on Si but not Li, and the kinetics of clay mineral formation structurally binding Si, while Li only substitutes for Mg or Ca, or adsorbs onto mineral surfaces (Pogge von Strandmann et al., 2012, 2017).

The co-variation of δ^{30}Si and δ^{7}Li is thus very strong for the mountainous west coast samples ($r^2 = 0.89$; Spearman correlation >95% significance), which are also samples with very low vegetation ($r^2 = 0.85$), but non-existent for the east coast floodplains (**Figure 4E**). This is expected, given that both plant (or algal) growth and clay formation are significantly greater on the east coast. In other words, the enhanced dissolution of primary silicates in mountainous regions causes a correlation of Li and Si isotopes (also observed in the Himalayan foothills; Pogge von Strandmann et al., 2017). This co-relationship between the two systems can be modeled using a Rayleigh relationship (Vigier et al., 2009; Pogge von Strandmann et al., 2012, 2014b, 2017; Murphy et al., 2019), and by assuming a continental crust starting composition (Savage et al., 2010; Sauzéat et al., 2015). Using a kaolinite fractionation factor of $\alpha = 0.979$ for Li isotopes (Pistiner and Henderson, 2003; Hindshaw et al., 2019), and of 0.9989 for Si isotopes (close to values for allophane, which is compositionally similar to kaolinite; Ziegler et al., 2005; Delstanche et al., 2009), we can model the co-isotopic behavior for the western samples with between 20 and 60% of Li and Si removal (**Figure 4E**). This implies that both Li and

Si in these samples are only being affected by primary silicate dissolution, and the formation of single type of clay mineral (or a combination of minerals with the same fractionation factors). Kaolinite has previously been reported as the dominant clay forming in rivers on South Island (Jacobson et al., 2003).

For the eastern samples no such co-variation exists (**Figure 4E**). These flatter floodplain areas are more fractionated for both Li and Si isotopes (implying relatively more clay formation, i.e., less congruent weathering due to longer water-tock interaction times), but either multiple secondary minerals with different fractionation factors are causing the isotopic fractionation, or Si isotopes are additionally being affected by uptake by plants and freshwater diatoms.

Riverine Calcium

Like Mg isotopes, but unlike Li, Si, and U isotopes, calcium isotopes are also lithology-dependent. Both carbonates and silicates have a relatively wide δ^{44}Ca range (Fantle and Tipper, 2014), but on the whole carbonates are isotopically lighter than silicates, which range from ∼0.5 to 1.8‰. Equally, plants also impose variable Ca isotope fractionation (Fantle and Tipper, 2014).

Rather like Mg isotopes, there is no evidence of simple mixing (**Figure 2C**), and no relationship between this study's δ^{44}Ca values and any proxies for carbonate vs. silicate dissolution such as Ca/Na, Ca/Mg or divalent to monovalent cation ratios. Further, as for Mg, there is no true distinction between rivers draining different lithologies (δ^{44}Ca = 0.78 ± 0.21‰, n = 7 for greywacke; 1.01 ± 0.34‰, n = 4 for schist; 0.69 ± 0.14‰, n = 5 for Cenozoic sediments; **Table 1**). Equally, if both Ca and Mg were being controlled by mixing between carbonate and silicate dissolution, there should be a positive correlation between δ^{44}Ca and δ^{26}Mg, because carbonates are isotopically light and silicates isotopically heavy for both systems (Tipper et al., 2006a, 2008; Mavromatis et al., 2012; Fantle and Tipper, 2014; Pogge von Strandmann et al., 2014a, 2019b; Geske et al., 2015; Perez-Fernandez et al., 2017). However, no such relationship is observed, and if anything, the data exhibit a poor negative co-variation (**Figure 4D**) that also has no relationship to vegetation type.

In contrast, the samples do show negative co-variations between δ^{44}Ca and both δ^{7}Li and δ^{30}Si (**Figure 4C**). For Li vs. Ca, this co-variation is only present in the western (mountainous) samples. Given that low δ^{7}Li and low δ^{30}Si values are caused by more congruent weathering (relatively more dissolution of primary silicates) (Pogge von Strandmann and Henderson, 2015), this implies that the silicate endmember for Ca isotopes would be isotopically fairly heavy. Applying the same Li and Si fractionation factors as for the δ^{7}Li–δ^{30}Si co-variation (**Figures 4A,B**) suggests that the δ^{44}Ca of the original silicate material must be ∼1.75‰. Although this is just within the global range of silicate rocks (Fantle and Tipper, 2014), no rock or mineral values that heavy have been reported from New Zealand (Moore et al., 2013). Overall, however, this trend toward isotopically heavy Ca isotope ratios with light Li or Si isotope ratios is only driven by a single sample, while the remaining rivers have δ^{44}Ca < 1.06‰, similar to those of Moore et al. (2013) from New Zealand. It is difficult to determine why this sample from the Whataroa river is so isotopically heavy. While carbonate precipitation could drive δ^{44}Ca to values even higher than observed here (Pogge von Strandmann et al., 2019a), the rivers of South Island have been reported to be undersaturated for carbonates, making it unlikely that they are precipitating (Moore et al., 2013). The other possibilities, therefore, are either the dissolution of an isotopically heavy material, or that the sample is dominated by precipitation with the composition of seawater (δ^{44}Ca ∼1.9‰). It has experimentally been observed that calcite dissolution can drive Ca isotope ratios to even isotopically heavier values than observed here, due to the attainment of dynamic mineral-fluid equilibrium (Oelkers et al., 2019b). However, this would be unlikely to cause light Li or Si isotope ratios. Alternatively, dissolution of silicate secondary weathering products (heavy for Ca isotopes, but light for Li and Si isotopes) and/or rainwater contribution could explain this sample. Some elemental ratios in this sample, such as Mg/Na, are identical to that of seawater, suggesting a considerable input from seawater aerosols via precipitation, potentially exacerbated by a high rainfall rate (Robinson et al., 2004). This would potentially decouple Ca from Si isotope ratios in this sample, given that precipitation contains very little Si.

Without this sample, the riverine δ^{44}Ca values are similar to other studies of New Zealand, which concluded that Ca is largely sourced from the dissolution of carbonates (Moore et al., 2013). However, given the lack of co-variation with Ca isotopes, it seems more likely that Ca isotopes are the result of mixing between carbonate and silicate dissolution, in some cases with an additional mixing component from the exchangeable fraction of shallow soils.

Finally, there is no co-variation between this study's δ^{44}Ca values and uplift (or supply) rate (**Figure 3D**), with fairly constant isotope ratios across the entire range of uplift rates. Hence, even if these samples are dominated by carbonates, its enhanced dissolution due to more rapid supply rates is not obvious from Ca isotope ratios.

CONCLUSIONS

This study has analyzed the isotope ratios of the major cations directly involved in the long-term carbon cycle (Mg, Si, and Ca) from rivers on South Island, New Zealand. These samples have previously been analyzed for Li isotopes and U activity ratios, which in both cases exhibited co-variations with the uplift rates, which are used as a proxy for the rock supply rate to dissolution.

Here, the isotope ratios of the major elements do not co-vary with the uplift rate, indicating more complex controlling processes, including lithology and biology, neither of which affect Li or U isotopes. Li and Si isotopes broadly co-vary, especially in the mountainous west of the island, suggesting that both isotopes are controlled by the ratio of primary silicate mineral dissolution to secondary mineral formation.

In contrast, Mg and Ca isotopes do not co-vary with any physical parameters (e.g., uplift or rainfall rates). Aside from one isotopically heavy sample for Ca, both isotope ratios exhibit fairly little variation. Mg isotopes suggest that the system is dominated by silicate weathering, with clay formation driving isotope ratios lighter. Ca isotopes are also largely controlled by the mix of

lithology. Given that neither Mg nor Ca isotopes co-vary with Li, Si, or U isotopes, it implies that any weathering signal is masked by lithological and biological controls.

Overall, unlike the isotopes of the trace elements Li and U, the isotopes of the major elements Mg, Ca, and Si, in this case, are less useful for determining chemical weathering characteristics. This is largely because multiple processes (e.g., lithology, biology, and secondary mineral formation) tend to affect major elements, in contrast to Li and U, which are controlled by single processes. This, therefore, confirms the adage that major elements have major problems when using them to try to understand weathering processes.

DATA AVAILABILITY

All datasets generated for this study are included in the manuscript/supplementary files.

AUTHOR CONTRIBUTIONS

PP analyzed Mg and Ca isotopes, and wrote the manuscript. KH and JH analyzed and interpreted Si isotopes. LR provided the samples and edited the manuscript.

FUNDING

Mg and Ca analyses were funded by NERC grant NE/I020571/2 and ERC Consolidator grant 682760 CONTROLPASTCO2 (PP). Si isotope analyses funded by a Royal Society URF grant UF120084 and ERC Starting grant 678371 ICY-LAB (KH and JH).

ACKNOWLEDGMENTS

Thanks to Christopher Pearce and another reviewer for constructive comments.

REFERENCES

Andersen, M. B., Erel, Y., and Bourdon, B. (2009). Experimental evidence for U-234-U-238 fractionation during granite weathering with implications for U-234/U-238 in natural waters. *Geochim. Cosmochim. Acta* 73, 4124–4141. doi: 10.1016/j.gca.2009.04.020

Barber, A., Lalonde, K., Mucci, A., and Gelinas, Y. (2014). The role of iron in the diagenesis of organic carbon and nitrogen in sediments: a long-term incubation experiment. *Mar. Chem.* 162, 1–9. doi: 10.1016/j.marchem.2014.02.007

Berner, R. A. (2003). The long-term carbon cycle, fossil fuels and atmospheric composition. *Nature* 426, 323–326. doi: 10.1038/nature02131

Berner, R. A., Lasaga, A. C., and Garrels, R. M. (1983). The carbonate-silicate geochemical cycle and its effect on atmospheric carbon-dioxide over the past 100 million years. *Am. J. Sci.* 283, 641–683. doi: 10.2475/ajs.283.7.641

Black, J. R., Yin, Q. Z., and Casey, W. H. (2006). An experimental study of magnesium-isotope fractionation in chlorophyll-a photosynthesis. *Geochim. Cosmochim. Acta* 70, 4072–4079. doi: 10.1016/j.gca.2006.06.010

Blättler, C. L., Jenkyns, H. C., Reynard, L. M., and Henderson, G. M. (2011). Significant increases in global weathering during Oceanic Anoxic Events 1a and 2 indicated by calcium isotopes. *Earth Planet. Sci. Lett.* 309, 77–88. doi: 10.1016/j.epsl.2011.06.029

Bolou-Bi, E. B., Poszwa, A., Leyval, C., and Vigier, N. (2010). Experimental determination of magnesium isotope fractionation during higher plant growth. *Geochim. Cosmochim. Acta* 74, 2523–2537. doi: 10.1016/j.gca.2010.02.010

Bolou-Bi, E. B., Vigier, N., Poszwa, A., Boudot, J.-P., and Dambrine, E. (2012). Effects of biogeochemical processes on magnesium isotope variations in a forested catchment in the Vosges Mountains (France). *Geochim. Cosmochim. Acta* 87, 341–355. doi: 10.1016/j.gca.2012.04.005

Brenot, A., Cloquet, C., Vigier, N., Carignan, J., and France-Lanord, C. (2008). Magnesium isotope systematics of the lithologically varied Moselle river basin, France. *Geochim. Cosmochim. Acta* 72, 5070–5089. doi: 10.1016/j.gca.2008.07.027

Cardinal, D., Alleman, L. Y., de Jong, J. T. M., Ziegler, K., and Andre, L. (2003). Isotopic composition of silicon measured by multicollector plasma source mass spectrometry in dry plasma mode. *J. Anal. At. Spectrom.* 18, 213–218. doi: 10.1039/b210109b

Cardinal, D., Gaillardet, J., Hughes, H. J., Opfergelt, S., and Andre, L. (2010). Contrasting silicon isotope signatures in rivers from the Congo Basin and the specific behaviour of organic-rich waters. *Geophys. Res. Lett.* 37:L12403. doi: 10.1029/2010GL043413

Chabaux, F., Riotte, J., and Dequincey, O. (2003). "U-Th-Ra fractionation during weathering and river transport," in *Uranium-Series Geochemistry*, eds B. Bourdon, G. M. Henderson, C. C. Lundstrom, and S. P. Turner (Geochemical Society and Mineralogical Society of America), 533–576.

Chapela Lara, M., Buss, H. L., Pogge von Strandmann, P. A. E., Schuessler, J. A., and Moore, O. W. (2017). The influence of critical zone processes on the Mg isotope budget in a tropical, highly weathered andesitic catchment. *Geochim. Cosmochim. Acta* 202, 77–100. doi: 10.1016/j.gca.2016.12.032

De la Rocha, C. L., Brzezinski, M. A., and DeNiro, M. J. (1997). Fractionation of silicon isotopes by marine diatoms during biogenic silica formation. *Geochim. Cosmochim. Acta* 61, 5051–5056. doi: 10.1016/S0016-7037(97)00300-1

De la Rocha, C. L., Brzezinski, M. A., and DeNiro, M. J. (2000). A first look at the distribution of the stable isotopes of silicon in natural waters. *Geochim. Cosmochim. Acta* 64, 2467–2477. doi: 10.1016/S0016-7037(00)00373-2

Delstanche, S., Opfergelt, S., Cardinal, D., Elsass, F., Andre, L., and Delvaux, B. (2009). Silicon isotopic fractionation during adsorption of aqueous monosilicic acid onto iron oxide. *Geochim. Cosmochim. Acta* 73, 923–934. doi: 10.1016/j.gca.2008.11.014

Ding, T., Jiang, S., Wan, D., Li, Y., Li, J., Song, H., et al. (1996). *Silicon Isotope Geochemistry*. Beijing: Geological Publishing House.

Fantle, M. S., and Tipper, E. T. (2014). Calcium isotopes in the global biogeochemical Ca cycle: implications for development of a Ca isotope proxy. *Earth Sci. Rev.* 129, 148–177. doi: 10.1016/j.earscirev.2013.10.004

Farkaš, J., Bohm, F., Wallmann, K., Blenkinsop, J., Eisenhauer, A., van Geldern, R., et al. (2007). Calcium isotope record of Phanerozoic oceans: implications for chemical evolution of seawater and its causative mechanisms. *Geochim. Cosmochim. Acta* 71, 5117–5134. doi: 10.1016/j.gca.2007.09.004

Fontorbe, G., De la Rocha, C. L., Chapman, H. J., and Bickle, M. J. (2013). The silicon isotopic composition of the Ganges and its tributaries. *Earth Planet. Sci. Lett.* 381, 21–30. doi: 10.1016/j.epsl.2013.08.026

Foster, G. L., Pogge von Strandmann, P. A. E., and Rae, J. W. B. (2010). The boron and magnesium isotopic composition of seawater. *Geochem. Geophys. Geosyst.* 11:Q08015. doi: 10.1029/2010GC003201

Frings, P. J., Clymans, W., Fontorbe, G., De la Rocha, C. L., and Conley, D. J. (2016). The continental Si cycle and its impact on the ocean Si isotope budget. *Chem. Geol.* 425, 12–36. doi: 10.1016/j.chemgeo.2016.01.020

Frings, P. J., Clymans, W., Fontorbe, G., Gray, W., Chakrapani, G. J., Conley, D. J., et al. (2015). Silicate weathering in the Ganges alluvial plain. *Earth Planet. Sci. Lett.* 427, 136–148. doi: 10.1016/j.epsl.2015.06.049

Gaillardet, J., Dupre, B., Louvat, P., and Allegre, C. J. (1999). Global silicate weathering and CO_2 consumption rates deduced from the chemistry of large rivers. *Chem. Geol.* 159, 3–30. doi: 10.1016/S0009-2541(99)00031-5

Geilert, S., Vroon, P. Z., Keller, N. S., Gudbrandsson, S., Stefansson, A., and van Bergen, M. J. (2015). Silicon isotope fractionation during silica precipitation from hot-spring waters: evidence from the Geysir geothermal field. *Geochim. Cosmochim. Acta* 164, 403–427. doi: 10.1016/j.gca.2015.05.043

Geological Map of New Zealand (2012). *GNS Science, Institute of Geological & Nuclear Sciences*.

Georg, R. B., Reynolds, B. C., Frank, M., and Halliday, A. N. (2006a). Mechanisms controlling the silicon isotopic compositions of river waters. *Earth Planet. Sci. Lett.* 249, 290–306. doi: 10.1016/j.epsl.2006.07.006

Georg, R. B., Reynolds, B. C., Frank, M., and Halliday, A. N. (2006b). New sample preparation techniques for the determination of Si isotopic compositions using MC-ICPMS. *Chem. Geol.* 235, 95–104. doi: 10.1016/j.chemgeo.2006.06.006

Georg, R. B., Reynolds, B. C., West, A. J., Burton, K. W., and Halliday, A. N. (2007). Silicon isotope variations accompanying basalt weathering in Iceland. *Earth Planet. Sci. Lett.* 261, 476–490. doi: 10.1016/j.epsl.2007.07.004

Georg, R. B., West, A. J., Basu, A. R., and Halliday, A. N. (2009). Silicon fluxes and isotope composition of direct groundwater discharge into the Bay of Bengal and the effect on the global ocean silicon isotope budget. *Earth Planet. Sci. Lett.* 283, 67–74. doi: 10.1016/j.epsl.2009.03.041

Geske, A., Goldstein, R. H., Mavromatis, V., Richter, D. K., Buhl, D., Kluge, T., et al. (2015). The magnesium isotope (δ26Mg) signature of dolomites. *Geochim. Cosmochim. Acta* 149, 131–151. doi: 10.1016/j.gca.2014.11.003

Gíslason, S. R., Oelkers, E., and Snorrason, A. (2006). Role of river-suspended material in the global carbon cycle. *Geology* 34, 49–52. doi: 10.1130/G22045.1

Gislason, S. R., Oelkers, E. H., Eiriksdottir, E. S., Kardjilov, M. I., Gisladottir, G., Sigfusson, B., et al. (2009). Direct evidence of the feedback between climate and weathering. *Earth Planet. Sci. Lett.* 277, 213–222. doi: 10.1016/j.epsl.2008.10.018

Halicz, L., Galy, A., Belshaw, N. S., and O'Nions, K. (1999). High-precision measurement of calcium isotopes in carbonates and related materials by multiple collector inductively coupled plasma mass spectrometry (MC-ICP-MS). *J. Anal. At. Spectrom.* 14, 1835–1838. doi: 10.1039/a906422b

Hathorne, E. C., and James, R. H. (2006). Temporal record of lithium in seawater: a tracer for silicate weathering? *Earth Planet. Sci. Lett.* 246, 393–406. doi: 10.1016/j.epsl.2006.04.020

Hatton, J. E., Hendry, K. R., Hawkings, J. R., Wadham, J. L., Kohler, T. J., Stibal, M., et al. (2019). Investigation of subglacial weathering under the Greenland Ice Sheet using silicon isotopes. *Geochim. Cosmochim. Acta* 247, 191–206. doi: 10.1016/j.gca.2018.12.033

Hawley, S. M., Pogge von Strandmann, P. A. E., Burton, K. W., Williams, H. M., and Gislason, S. R. (2017). Continental weathering and terrestrial (oxyhydr)oxide export: comparing glacial and non-glacial catchments in Iceland. *Chem. Geol.* 462, 55–66. doi: 10.1016/j.chemgeo.2017.04.026

Henderson, G. M. (2002). Seawater (U-234/U-238) during the last 800 thousand years. *Earth Planet. Sci. Lett.* 199, 97–110. doi: 10.1016/S0012-821X(02)00556-3

Hendry, K. R., Leng, M. J., Robinson, L. F., Sloane, H. J., Blusztian, J., Rickaby, R. E. M., et al. (2011). Silicon isotopes in Antarctic sponges: an interlaboratory comparison. *Antarctic Sci.* 23, 34–42. doi: 10.1017/S0954102010000593

Higgins, J. A., and Schrag, D. P. (2010). Constraining magnesium cycling in marine sediments using magnesium isotopes. *Geochim. Cosmochim. Acta* 74, 2039–5053. doi: 10.1016/j.gca.2010.05.019

Hilley, G. E., Chamberlain, C. P., Moon, S., Porder, S., and Willett, S. D. (2010). Competition between erosion and reaction kinetics in controlling silicate-weathering rates. *Earth Planet. Sci. Lett.* 293, 191–199. doi: 10.1016/j.epsl.2010.01.008

Hin, R. C., Coath, C. D., Carter, P. J., Nimmo, F., Lai, Y. J., Pogge von Strandmann, P. A. E., et al. (2017). Magnesium isotope evidence that accretional vapour loss shapes planetary compositions. *Nature* 549, 511–515. doi: 10.1038/nature23899

Hindshaw, R. S., Aciego, S. M., and Tipper, E. T. (2018). Li and U isotopes as a potential tool for monitoring active layer deepening in permafrost dominated catchments. *Front. Earth Sci.* 6:102. doi: 10.3389/feart.2018.00102

Hindshaw, R. S., Bourdon, B., Pogge von Strandmann, P. A. E., Vigier, N., and Burton, K. W. (2013). The stable calcium isotopic composition of rivers draining basaltic catchments in Iceland. *Earth Planet. Sci. Lett.* 374, 173–184. doi: 10.1016/j.epsl.2013.05.038

Hindshaw, R. S., Tosca, R., Gout, T. L., Farnan, I., Tosca, N. J., and Tipper, E. T. (2019). Experimental constraints on Li isotope fractionation during clay formation. *Geochim. Cosmochim. Acta* 250, 219–237. doi: 10.1016/j.gca.2019.02.015

Hippler, D., Buhl, D., Witbaard, R., Richter, D. K., and Immenhauser, A. (2009). Towards a better understanding of magnesium-isotope ratios from marine skeletal carbonates. *Geochim. Cosmochim. Acta* 73, 6134–6146. doi: 10.1016/j.gca.2009.07.031

Hippler, D., Schmitt, A.-D., Gussone, N., Heuser, A., Stille, P., Eisenhauer, A., et al. (2003). Calcium isotopic composition of various reference materials and seawater. *Geostand. Newslett.* 27, 13–19. doi: 10.1111/j.1751-908X.2003.tb00709.x

Holland, H. D. (2005). Sea level, sediments and the composition of seawater. *Am. J. Sci.* 305, 220–239. doi: 10.2475/ajs.305.3.220

Holmden, C., Panchuk, K., and Finney, S. C. (2012). Tightly coupled records of Ca and C isotope changes during the Hirnantian glaciation event in an epeiric sea setting. *Geochim. Cosmochim. Acta* 98, 94–106. doi: 10.1016/j.gca.2012.09.017

Huang, K. J., Teng, F. Z., Wei, G. J., Ma, J. L., and Bao, Z. Y. (2012). Adsorption- and desorption-controlled magnesium isotope fractionation during extreme weathering of basalt in Hainan Island, China. *Earth Planet. Sci. Lett.* 359–360, 73–83. doi: 10.1016/j.epsl.2012.10.007

Hughes, H. J., Delvigne, C., Korntheuer, M., de Jong, J. T. M., Andre, L., and Cardinal, D. (2011). Controlling the mass bias introduced by anionic and organic matrices in silicon isotopic measurements by MC-ICP-MS. *J. Anal. At. Spectrom.* 26, 1892–1896. doi: 10.1039/c1ja10110b

Jacobson, A. D., Andrews, M. G., Lehn, G. O., and Holmden, C. (2015). Silicate versus carbonate weathering in Iceland: new insights from Ca isotopes. *Earth Planet. Sci. Lett.* 416, 132–142. doi: 10.1016/j.epsl.2015.01.030

Jacobson, A. D., and Blum, J. D. (2003). Relationship between mechanical erosion and atmospheric CO_2 consumption in the New Zealand Southern Alps. *Geology* 31, 865–868. doi: 10.1130/G19662.1

Jacobson, A. D., Blum, J. D., Chamberlain, C. P., Craw, D., and Koons, P. O. (2003). Climatic and tectonic controls on chemical weathering in the New Zealand Southern Alps. *Geochim. Cosmochim. Acta* 67, 29–46. doi: 10.1016/S0016-7037(02)01053-0

Kasemann, S. A., Hawkesworth, C., Prave, A. R., Fallick, A. E., and Pearson, P. N. (2005). Boron and calcium isotope composition in Neoproterozoic carbonate rocks from Namibia: evidence for extreme environmental change. *Earth Planet. Sci. Lett.* 231, 73–86. doi: 10.1016/j.epsl.2004.12.006

Kasemann, S. A., Pogge von Strandmann, P. A. E., Prave, A. R., Fallick, A. E., Elliott, T., and Hoffmann, K. H. (2014). Continental weathering following a Cryogenian glaciation: evidence from calcium and magnesium isotopes. *Earth Planet. Sci. Lett.* 396, 66–77. doi: 10.1016/j.epsl.2014.03.048

Kasemann, S. A., Schmidt, D. N., Pearson, N. J., and Hawkesworth, C. J. (2008). Biological and ecological insights into Ca isotopes in planktic foraminifers as a palaeotemperature proxy. *Earth Planet. Sci. Lett.* 271, 292–302. doi: 10.1016/j.epsl.2008.04.007

Lalonde, K., Mucci, A., Ouellet, A., and Gelinas, Y. (2012). Preservation of organic matter in sediments promoted by iron. *Nature* 483, 198–200. doi: 10.1038/nature10855

Lee, S.-W., Ryu, J.-S., and Lee, K.-S. (2014). Magnesium isotope geochemistry in the Han River, South Korea. *Chem. Geol.* 364, 9–19. doi: 10.1016/j.chemgeo.2013.11.022

Li, G., and West, A. J. (2014). Evolution of Cenozoic seawater lithium isotopes: coupling of global denudation regime and shifting seawater sinks. *Earth Planet. Sci. Lett.* 401, 284–293. doi: 10.1016/j.epsl.2014.06.011

Liu, X.-L., Teng, F. Z., Rudnick, R. L., McDonough, W. F., and Cummings, M. L. (2014). Massive magnesium depletion and isotope fractionation in weathered basalts. *Geochim. Cosmochim. Acta* 135, 336–349. doi: 10.1016/j.gca.2014.03.028

Mavromatis, V., Pearce, C. R., Shirokova, L. S., Bundeleva, I. A., Pokrovsky, O. S., Benezeth, P., et al. (2012). Magnesium isotope fractionation during hydrous magnesium carbonate precipitation with and without cyanobacteria. *Geochim. Cosmochim. Acta* 76, 161–174. doi: 10.1016/j.gca.2011.10.019

McArthur, J. M., Howarth, R. J., and Bailey, T. R. (2001). Strontium isotope stratigraphy: LOWESS version 3: best fit to the marine Sr-isotope curve for 0-509 Ma and accompanying look-up table for deriving numerical age. *J. Geol.* 109, 155–170. doi: 10.1086/319243

Misra, S., and Froelich, P. N. (2012). Lithium isotope history of cenozoic seawater: changes in silicate weathering and reverse weathering. *Science* 335, 818–823. doi: 10.1126/science.1214697

Moore, J., Jacobson, A. D., Holmden, C., and Craw, D. (2013). Tracking the relationship between mountain uplift, silicate weathering, and long-term CO_2 consumption with Ca isotopes: Southern Alps, New Zealand. *Chem. Geol.* 341, 110–127. doi: 10.1016/j.chemgeo.2013.01.005

Murphy, M. J., Porcelli, D., Pogge von Strandmann, P. A. E., Hirst, C. A., Kutscher, L., Katchinoff, J. A., et al. (2019). Tracing silicate weathering processes in the permafrost-dominated Lena River watershed using lithium isotopes. *Geochim. Cosmochim. Acta* 245, 154–171. doi: 10.1016/j.gca.2018.10.024

Oelkers, E. H., Butcher, R., Pogge von Strandmann, P. A. E., Schuessler, J. A., von Blanckenburg, F., Snaebjornsdottir, S. O., et al. (2019a). Using stable Mg isotope signatures to assess the fate of magnesium during the *in situ* mineralisation of CO_2 and H2S at the CarbFix site in SW-Iceland. *Geochim. Cosmochim. Acta* 245, 542–555. doi: 10.1016/j.gca.2018.11.011

Oelkers, E. H., Pogge von Strandmann, P. A. E., and Mavromatis, V. (2019b). The rapid resetting of the Ca isotopic signatures of calcite at ambient temperature during its congruent dissolution, precipitation, and at equilibrium. *Chem. Geol.* 512, 1–10. doi: 10.1016/j.chemgeo.2019.02.035

Opfergelt, S., Burton, K. W., Georg, R. B., West, A. J., Guicharnaud, R. A., Sigfusson, B., et al. (2014). Magnesium retention on the soil exchange complex controlling Mg isotope variations in soils, soil solutions and vegetation in volcanic soils, Iceland. *Geochim. Cosmochim. Acta* 125, 110–130. doi: 10.1016/j.gca.2013.09.036

Opfergelt, S., Burton, K. W., Pogge von Strandmann, P. A. E., Gislason, S. R., and Halliday, A. N. (2013). Riverine silicon isotope variations in glaciated basaltic terrains: implications for the Si delivery to the ocean over glacial–interglacial intervals. *Earth Planet. Sci. Lett.* 369–370, 211–219. doi: 10.1016/j.epsl.2013.03.025

Opfergelt, S., Cardinal, D., Henriet, C., Drave, X., Andre, L., and Delvaux, B. (2006). Silicon isotopic fractionation by banana (*Musa* spp.) grown in a continuous nutrient flow device. *Plant Soil* 285, 333–345. doi: 10.1007/s11104-006-9019-1

Opfergelt, S., de Bournonville, G., Cardinal, D., Andre, L., Delstanche, S., and Delvaux, B. (2009). Impact of soil weathering degree on silicon isotopic fractionation during adsorption onto iron oxides in basaltic ash soils, Cameroon. *Geochim. Cosmochim. Acta* 73, 7226–7240. doi: 10.1016/j.gca.2009.09.003

Opfergelt, S., Eiriksdottir, E. S., Burton, K. W., Einarsson, A., Siebert, C., Gislason, S. R., et al. (2011). Quantifying the impact of freshwater diatom productivity on silicon isotopes and silicon fluxes: Lake Myvatn, Iceland. *Earth Planet. Sci. Lett.* 305, 73–82. doi: 10.1016/j.epsl.2011.02.043

Opfergelt, S., Georg, R. B., Delvaux, B., Cabidoche, Y. M., Burton, K. W., and Halliday, A. N. (2012a). Mechanisms of magnesium isotope fractionation in volcanic soil weathering sequences, Guadeloupe. *Earth Planet. Sci. Lett.* 341, 176–185. doi: 10.1016/j.epsl.2012.06.010

Opfergelt, S., Georg, R. B., Delvaux, B., Cabidoche, Y. M., Burton, K. W., and Halliday, A. N. (2012b). Silicon isotopes and the tracing of desilication in volcanic soil weathering sequences, Guadeloupe. *Chem. Geol.* 326, 113–122. doi: 10.1016/j.chemgeo.2012.07.032

Opfergelt, S., Williams, H. M., Cornelis, J. T., Guicharnaud, R. A., Georg, R. B., Siebert, C., et al. (2017). Iron and silicon isotope behaviour accompanying weathering in Icelandic soils, and the implications for iron export from peatlands. *Geochim. Cosmochim. Acta* 217, 273–291. doi: 10.1016/j.gca.2017.08.033

Panizzo, V. N., Swann, G. E. A., Mackay, A. W., Vologina, E., Sturm, M., Pashley, V., et al. (2016). Insights into the transfer of silicon isotopes into the sediment record. *Biogeosciences* 13, 147–157. doi: 10.5194/bg-13-147-2016

Perez-Fernandez, A., Berninger, U.-N., Mavromatis, V., Pogge von Strandmann, P. A. E., and Oelkers, E. H. (2017). Ca and Mg isotope fractionation during the stoichiometric dissolution of dolomite at temperatures from 51 to 126°C and 5 bars CO_2 pressure. *Chem. Geol.* 467, 76–88. doi: 10.1016/j.chemgeo.2017.07.026

Pistiner, J. S., and Henderson, G. M. (2003). Lithium-isotope fractionation during continental weathering processes. *Earth Planet. Sci. Lett.* 214, 327–339. doi: 10.1016/S0012-821X(03)00348-0

Pogge von Strandmann, P. A. E., Burton, K. W., James, R. H., van Calsteren, P., and Gislason, S. R. (2008). The influence of weathering processes on riverine magnesium isotopes in a basaltic terrain. *Earth Planet. Sci. Lett.* 276, 187–197. doi: 10.1016/j.epsl.2008.09.020

Pogge von Strandmann, P. A. E., Burton, K. W., James, R. H., van Calsteren, P., and Gislason, S. R. (2010). Assessing the role of climate on uranium and lithium isotope behaviour in rivers draining a basaltic terrain. *Chem. Geol.* 270, 227–239. doi: 10.1016/j.chemgeo.2009.12.002

Pogge von Strandmann, P. A. E., Burton, K. W., James, R. H., van Calsteren, P., Gislason, S. R., and Mokadem, F. (2006). Riverine behaviour of uranium and lithium isotopes in an actively glaciated basaltic terrain. *Earth Planet. Sci. Lett.* 251, 134–147. doi: 10.1016/j.epsl.2006.09.001

Pogge von Strandmann, P. A. E., Burton, K. W., Porcelli, D., James, R. H., van Calsteren, P., and Gislason, S. R. (2011a). Transport and exchange of U-series nuclides between suspended material, dissolved load and colloids in rivers draining basaltic terrains. *Earth Planet. Sci. Lett.* 301, 125–136. doi: 10.1016/j.epsl.2010.10.029

Pogge von Strandmann, P. A. E., Burton, K. W., Snaebjornsdottir, S. O., Sigfusson, B., Aradottir, E. S. P., Gunnarsson, I., et al. (2019a). Rapid CO_2 mineralisation into calcite at the CarbFix storage site quantified using calcium isotopes. *Nat Commun.* 10:1983. doi: 10.1038/s41467-019-10003-8

Pogge von Strandmann, P. A. E., Elliott, T., Marschall, H. R., Coath, C., Lai, Y. J., Jeffcoate, A. B., et al. (2011b). Variations of Li and Mg isotope ratios in bulk chondrites and mantle xenoliths. *Geochim. Cosmochim. Acta* 75, 5247–5268. doi: 10.1016/j.gca.2011.06.026

Pogge von Strandmann, P. A. E., Forshaw, J., and Schmidt, D. N. (2014a). Modern and Cenozoic records of seawater magnesium from foraminiferal Mg isotopes. *Biogeosciences* 11, 5155–5168. doi: 10.5194/bg-11-5155-2014

Pogge von Strandmann, P. A. E., Frings, P. J., and Murphy, M. J. (2017). Lithium isotope behaviour during weathering in the Ganges Alluvial Plain. *Geochim. Cosmochim. Acta* 198, 17–31. doi: 10.1016/j.gca.2016.11.017

Pogge von Strandmann, P. A. E., and Henderson, G. M. (2015). The Li isotope response to mountain uplift. *Geology* 43, 67–70. doi: 10.1130/G36162.1

Pogge von Strandmann, P. A. E., Olsson, J., Luu, T.-H., Gislason, S. R., and Burton, K. W. (2019b). Using Mg isotopes to estimate natural calcite compositions and precipitation rates during the 2010 Eyjafjallajökull eruption. *Front. Earth Sci.* 7:6. doi: 10.3389/feart.2019.00006

Pogge von Strandmann, P. A. E., Opfergelt, S., Lai, Y. J., Sigfusson, B., Gislason, S. R., and Burton, K. W. (2012). Lithium, magnesium and silicon isotope behaviour accompanying weathering in a basaltic soil and pore water profile in Iceland. *Earth Planet. Sci. Lett.* 339–340, 11–23. doi: 10.1016/j.epsl.2012.05.035

Pogge von Strandmann, P. A. E., Porcelli, D., James, R. H., van Calsteren, P., Schaefer, B. F., Cartwright, I., et al. (2014b). Chemical weathering processes in the Great Artesian Basin: evidence from lithium and silicon isotopes. *Earth Planet. Sci. Lett.* 406, 24–36. doi: 10.1016/j.epsl.2014.09.014

Ravizza, G. (1993). Variations of the Os-187/Os-186 ratio of seawater over the past 28 million years as inferred from metalliferous carbonates. *Earth Planet. Sci. Lett.* 118, 335–348. doi: 10.1016/0012-821X(93)90177-B

Raymo, M. E., and Ruddiman, W. F. (1992). Tectonic forcing of late cenozoic climate. *Nature* 359, 117–122. doi: 10.1038/359117a0

Raymo, M. E., Ruddiman, W. F., and Froelich, P. N. (1988). Influence of late Cenozoic mountain building on ocean geochemical cycles. *Geology* 16, 649–653. doi: 10.1130/0091-7613(1988)016<0649:IOLCMB>2.3.CO;2

Reynard, L. M., Day, C. C., and Henderson, G. M. (2010). Large fractionation of calcium isotopes during cave-analogue calcium carbonate growth. *Geochim. Cosmochim. Acta* 75, 3726–3740. doi: 10.1016/j.gca.2011.04.010

Reynolds, B. C., Aggarwal, P. K., Andre, L., Baxter, D. C., Beucher, C., Brzezinski, M. A., et al. (2007). An inter-laboratory comparison of Si isotope reference materials. *J. Anal. At. Spectrom.* 22, 561–568. doi: 10.1039/B616755A

Robinson, L. F., Henderson, G. M., Hall, L., and Matthews, I. (2004). Climatic control of riverine and Seawater uranium-isotope ratios. *Science* 305, 851–854. doi: 10.1126/science.1099673

Sauzéat, L., Rudnick, R. L., Chauvel, C., Garcon, M., and Tang, M. (2015). New perspectives on the Li isotopic composition of the upper continental crust and its weathering signature. *Earth Planet. Sci. Lett.* 428, 181–192. doi: 10.1016/j.epsl.2015.07.032

Savage, P. S., Georg, R. B., Armytage, R. M. G., Williams, H. M., and Halliday, A. N. (2010). Silicon isotope homogeneity in the mantle. *Earth Planet. Sci. Lett.* 295, 139–146. doi: 10.1016/j.epsl.2010.03.035

Schrumpf, M., Kaiser, K., Guggenberger, G., Persson, T., Kogel-Knabner, I., and Schulze, E.-D. (2013). Storage and stability of organic carbon in soils as related to depth, occlusion within aggregates and attachment to minerals. *Biogeosciences* 10, 1675–1691. doi: 10.5194/bg-10-1675-2013

Shalev, N., Farkas, J., Fietzke, J., Novak, M., Schuessler, J. A., Pogge von Strandmann, P. A. E., et al. (2018). Mg isotope inter-laboratory comparison of reference materials from earth-surface low-temperature

environments. *Geostand. Geoanalyt. Res.* 42, 105–221. doi: 10.1111/ggr.12208

Teng, F. Z. (2017). Magnesium isotope geochemistry. *Rev. Min. Geochem.* 82, 219–287. doi: 10.2138/rmg.2017.82.7

Teng, F. Z., Li, W. Y., Rudnick, R. L., and Gardner, L. R. (2010). Contrasting lithium and magnesium isotope fractionation during continental weathering. *Earth Planet. Sci. Lett.* 300, 63–71. doi: 10.1016/j.epsl.2010.09.036

Teng, F. Z., Yin, Q. Z., Ullmann, C. V., Chakrabarti, R., Pogge von Strandmann, P. A. E., Yang, W., et al. (2015). Interlaboratory comparison of magnesium isotopic compositions of 12 felsic to ultramafic igneous rock standards analyzed by MC-ICPMS. *Geochem. Geophys. Geosyst.* 16, 3197-3209. doi: 10.1002/2015GC005939

Tipper, E. T., Calmels, D., Gaillardet, J., Louvat, P., Capmas, F., and Dubacq, B. (2012a). Positive correlation between Li and Mg isotope ratios in the river waters of the Mackenzie Basin challenges the interpretation of apparent isotopic fractionation during weathering. *Earth Planet. Sci. Lett.* 333, 35–45. doi: 10.1016/j.epsl.2012.04.023

Tipper, E. T., Gaillardet, J., Louvat, P., Capmas, F., and White, A. F. (2010). Mg isotope constraints on soil pore-fluid chemistry: evidence from Santa Cruz, California. *Geochim. Cosmochim. Acta* 74, 3883–3896. doi: 10.1016/j.gca.2010.04.021

Tipper, E. T., Galy, A., and Bickle, M. (2008). Calcium and magnesium isotope systematics in rivers draining the Himalaya-Tibetan-Plateau region: lithological or fractionation control? *Geochim. Cosmochim. Acta* 72, 1057–1075. doi: 10.1016/j.gca.2007.11.029

Tipper, E. T., Galy, A., and Bickle, M. J. (2006a). Riverine evidence for a fractionated reservoir of Ca and Mg on the continents: implications for the oceanic Ca cycle. *Earth Planet. Sci. Lett.* 247, 267–279. doi: 10.1016/j.epsl.2006.04.033

Tipper, E. T., Galy, A., Gaillardet, J., Bickle, M. J., Elderfield, H., and Carder, E. A. (2006b). The magnesium isotope budget of the modern ocean: constraints from riverine magnesium isotope ratios. *Earth Planet. Sci. Lett.* 250, 241–253. doi: 10.1016/j.epsl.2006.07.037

Tipper, E. T., Lemarchand, E., Hindshaw, R. S., Reynolds, B. C., and Bourdon, B. (2012b). Seasonal sensitivity of weathering processes: hints from magnesium isotopes in a glacial stream. *Chem. Geol.* 312–313, 80–92. doi: 10.1016/j.chemgeo.2012.04.002

Tranter, M., Sharp, M. J., Lamb, H. R., Brown, G. H., Hubbard, B. P., and Willis, I. C. (2002). Geochemical weathering at the bed of Haut Glacier d'Arolla, Switzerland - a new model. *Hydrol. Process.* 16, 959–993. doi: 10.1002/hyp.309

Vigier, N., Gislason, S. R., Burton, K. W., Millot, R., and Mokadem, F. (2009). The relationship between riverine lithium isotope composition and silicate weathering rates in Iceland. *Earth Planet. Sci. Lett.* 287, 434–441. doi: 10.1016/j.epsl.2009.08.026

Walker, J. C. G., Hays, P. B., and Kasting, J. F. (1981). A negative feedback mechanism for the long-term stabilization of earths surface-temperature. *J. Geophys. Res. Oceans Atmos.* 86, 9776–9782. doi: 10.1029/JC086iC10p09776

Wanner, C., Sonnenthal, E. L., and Liu, X.-M. (2014). Seawater δ7Li: a direct proxy for global CO_2 consumption by continental silicate weathering? *Chem. Geol.* 381, 154–167. doi: 10.1016/j.chemgeo.2014.05.005

West, A. J., Bickle, M. J., Collins, R., and Brasington, J. (2002). Small-catchment perspective on Himalayan weathering fluxes. *Geology* 30, 355–358. doi: 10.1130/0091-7613(2002)030<0355:SCPOHW>2.0.CO;2

West, A. J., Galy, A., and Bickle, M. (2005). Tectonic and climatic controls on silicate weathering. *Earth Planet. Sci. Lett.* 235, 211–228. doi: 10.1016/j.epsl.2005.03.020

Wimpenny, J., Burton, K. W., James, R. H., Gannoun, A., Mokadem, F., and Gislason, S. R. (2011). The behaviour of magnesium and its isotopes during glacial weathering in an ancient shield terrain in West Greenland. *Earth Planet. Sci. Lett.* 304, 260–269. doi: 10.1016/j.epsl.2011.02.008

Wimpenny, J., Colla, C. A., Yin, Q. Z., Rustad, J. R., and Casey, W. H. (2014). Investigating the behaviour of Mg isotopes during the formation of clay minerals. *Geochim. Cosmochim. Acta* 128, 178–194. doi: 10.1016/j.gca.2013.12.012

Wombacher, F., Eisenhauer, A., Bohm, F., Gussone, N., Regenberg, M., Dullo, W. C., et al. (2011). Magnesium stable isotope fractionation in marine biogenic calcite and aragonite. *Geochim. Cosmochim. Acta* 75, 5797–5818. doi: 10.1016/j.gca.2011.07.017

Ziegler, K., Chadwick, O. A., Brzezinski, M. A., and Kelly, E. F. (2005). Natural variations of delta Si-30 ratios during progressive basalt weathering, Hawaiian Islands. *Geochim. Cosmochim. Acta* 69, 4597–4610. doi: 10.1016/j.gca.2005.05.008

Conflict of Interest Statement: The authors declare that the research was conducted in the absence of any commercial or financial relationships that could be construed as a potential conflict of interest.